Oxygen ordering in $YBa_2Cu_3O_{6+x}$: low-temperature expansions

Oxygen ordering in $YBa_2Cu_3O_{6+x}$: low-temperature expansions

J Oitmaa†, Yang Jie†§ and L T Wille‡

† School of Physics, The University of New South Wales, Kensington, NSW 2033, Australia
‡ Department of Physics, Florida Atlantic University, Boca Raton, FL 33431, USA

Abstract. Low-temperature series expansions are used to investigate the phase transition due to oxygen ordering in the high-temperature superconductor $YBa_2Cu_3O_{6+x}$. The formulation is based on the lattice-gas model, which has been studied by many authors, and excellent agreement with previous results is obtained. We also investigate the effect of a sublattice-dependent chemical potential which plays a role similar to a uniaxial stress in breaking the degeneracy between twinned structures.

1. Introduction

One of the interesting aspects of the high-temperature superconductor $YBa_2Cu_3O_{6+x}$ is the role played by the variable oxygen content, both on the structural properties at high temperature and on the superconducting transition itself.

The structure of the material is by now well known [1], and consists of layers of fixed stoichiometry as well as, in each unit cell, a particular layer which has variable oxygen content. In accordance with common usage we refer to these as the 'CuO planes'. Each CuO plane, shown in figure 1(a), consists of an approximately square network of Cu ions separated by O sites. At $x = 0, 1$ the O sites are respectively empty and half-filled. The material can exist in a high-temperature tetragonal phase, in which the oxygen sites are occupied randomly and an orthorhombic phase in which the oxygens are, at least partially, ordered in parallel chains. Such structures are shown in figures 1(b), (c). The tetragonal–orthorhombic structural phase transition depends on the oxygen content and occurs at 900–1000 K. The superconducting transition temperature also correlates with oxygen content [2, 3] but the basis for this relationship is not clear.

From a variety of experiments we may then infer a phase diagram in the (x, T) and (μ, T) planes which, at least qualitatively, has the form shown in figure 2. De Fontaine *et al* [4] proposed a lattice-gas model to represent the essential physics of the oxygen ordering. The model has three separate interactions, represented by effective pair energies V_1, V_2, V_3 as shown in figure 3. The interactions V_1 and V_3 are assumed to be repulsive whereas V_2, which is mediated by an intervening Cu ion, is attractive. This follows from an analysis of the ground-state phase diagram of the model [5]. Other models have also been proposed, notably those of Khachaturyan *et al* [6], Aligia *et al* [7], and Zubkus *et al* [8]. A large number of studies of this model have been reported [9–17], using Monte Carlo simulations, cluster-variation calculations and transfer matrix calculations. Broadly speaking agreement

§ Present address: Institute of Physics, Chinese Academy of Sciences, Beijing 100080, People's Republic of China.
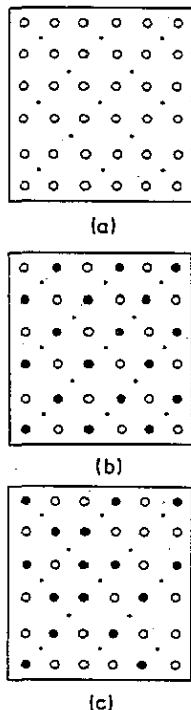
Figure 1. (*a*) Structure of the CuO plane. The small dots are filled Cu sites, the large circles are O sites, which may be filled or empty. (*b*) The fully ordered structure with $x = 1$. (*c*) A general configuration showing partial order and twinning.

with the schematic phase diagram is obtained, although a number of open questions remain. Among these are the nature of the transition at low T, the existence of an equilibrium phase (anti-Ortho I) at low x, and the possible existence of other equilibrium structures with different periodicities. The existence of such structures is not predicted by this model, and requires the inclusion of longer range interactions [7, 18, 19].

We have investigated this model by the method of low-temperature expansions [20, 21]. We report results for the Ortho I–Tetra transition line, our numerical values being in close agreement with previous work. In addition we model the effect of uniaxial stress on the material, which is often applied during growth to prevent twinning [22–24], and we estimate the change in transition temperature which results.

2. Low-temperature expansions

Derivation of low-temperature expansions for any system, where the ground state is known and the excited states and their excitation energies can be enumerated, starts from the expression

$$\frac{1}{N} \ln Z = -\beta E_0 + \sum_{\{G\}} a_G e^{-\beta \Delta E_G}. \tag{1}$$

Here E_0 is the ground-state energy per site and the summation is over excited states, which we identify with graphs on the lattice. a_G is the usual 'strong' lattice constant of the graph [20], ΔE_G is the corresponding excitation energy, and $\beta = 1/kT$ as usual. Thus an expansion is associated with a particular ordered state and different regions of the phase diagram will lead to different expansions.
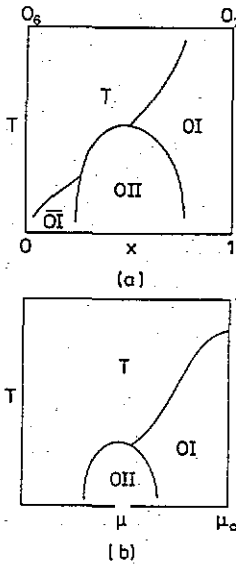
Figure 2. Schematic phase diagram (*a*) in the *x–T* plane, and (*b*) in the *μ–T* plane. μ_0 corresponds to $h = 0$, about which the phase diagram is symmetric. Predicted equilibrium phases are T (tetragonal), OI (orthorhombic I), OII (orthorhombic II), and $\overline{\text{OI}}$. For a full description of these phases see [17].
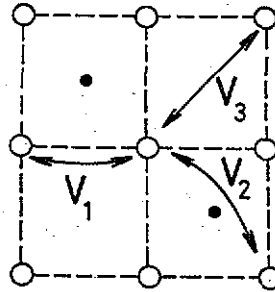

Figure 3. The lattice-gas model with interactions V_1, V_2, V_3.

The lattice-gas Hamiltonian [4] is

$$H = V_1 \sum_{(1)} n_i n_j + V_2 \sum_{(2)} n_i n_j + V_3 \sum_{(3)} n_i n_j - \mu \sum_i n_i \tag{2}$$

where $n_i = 0,1$ is an occupation number at site i, μ is the chemical potential, and the summations are over the appropriate pairs. It is convenient, though not essential, to write (2) in terms of Ising variables $\sigma_i = \pm 1$, via $n_i = (1 - \sigma_i)/2$, so that an unoccupied site has spin up. The Hamiltonian becomes

$$H = N\epsilon_0 + J_1 \sum_{(1)} \sigma_i \sigma_j + J_2 \sum_{(2)} \sigma_i \sigma_j + J_3 \sum_{(3)} \sigma_i \sigma_j - h \sum_i \sigma_i \tag{3}$$

with $J_i = V_i/4$ and $h = (2V_1 + V_2 + V_3 - \mu)/2$. This is an Ising model with nearest-neighbour antiferromagnetic interactions, anisotropic next-nearest-neighbour interactions, with an external magnetic field h.

In this paper we choose the ground state of the system to be one of the two degenerate Néel states, with $\sigma = -1, +1$ on sublattices A, B respectively. In lattice-gas language this is the fully ordered $x = 1$ configuration, with all sites on sublattice A occupied and all sites on sublattice B empty. For any perturbed configuration the energy change can be expressed as

$$\Delta E = 4p_1 J_1 + 4p_2 |J_2| + 4p_3 J_3 + 2p_4 h \tag{4}$$

where p_1, p_2, p_3, p_4 are integers defined by $p_1 = 2r - s_1$, $p_2 = r - s_2$, $p_3 = r - s_3$, $p_4 = 2r_A - r$ with r = number of overturned spins from ground state, r_A = number of

Graph	Lattice Constant	P_1	P_2	P_3	P_4
o	1/2	2	1	1	1
●	1/2	2	1	1	-1
●——o	2	3	2	2	0
●-x-●	1/2	4	1	2	-2
●---●	1/2	4	2	1	-2
o-x-o	1/2	4	1	2	2
o---o	1/2	4	2	1	2
o o	-5/4	4	2	2	2
o ●	-2	4	2	2	0
● ●	-5/4	4	2	2	-2

Notation:

o   overturned spin on sublattice 1

●   overturned spin on sublattice 2

———   bond of type J_1 (V_1)

--x--   bond of type J_2 (V_2)

-----   bond of type J_3 (V_3)

Figure 4. Low-order perturbed configurations and corresponding expansion parameters.
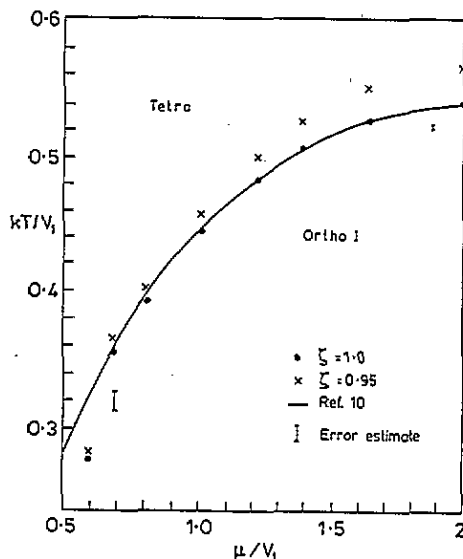
Figure 5. The Ortho I–Tetra phase boundary as obtained from low-temperature series, for the cases $\zeta = 1.0$ (uniform chemical potential) and $\zeta = -0.95$. For comparison the transfer matrix results [17] are also shown.

overturned spins on sublattice A and s_i = number of bonds of type i ($i = 1,2,3$) in the cluster of overturned spins.

In figure 4 we list the lowest few perturbed configurations with their lattice constants a_G and descriptors $\{p_i\}$.

To determine the phase boundary for the model it is necessary to compute series for the order parameter and/or for the ordering susceptibility. For this reason we include a 'staggered field' in the Ising Hamiltonian

$$H' = H - h_s \sum_i \eta_i \sigma_i \tag{5}$$

with $\eta_i = +1, -1$ for sublattice A, B respectively.

The expansion for the free energy per spin can finally be expressed in the form

$$-\beta f = -\beta E_0 + \sum_r L_r(u_1, u_2, u_3, y) y_s^r \tag{6}$$

with

$$L_r = \sum_{\{p\}} C_r\{p\} u_1^{p_1} u_2^{p_2} u_3^{p_3} y^{p_4} \tag{7}$$

$$u_1 = e^{-\beta V_1} \qquad u_2 = e^{-\beta |V_2|} \qquad u_3 = e^{\beta V_3} \qquad y = e^{-2\beta h} \qquad y_s = e^{-2\beta h_s}.$$

The series for the order parameter (staggered magnetization) and ordering susceptibility are then obtained from (6) as

$$M_s = \frac{1}{\beta} \lim_{h_s \to 0} \frac{\partial}{\partial h_s} (-\beta f) = 1 - 2 \sum_{r=1}^{\infty} r L_r(u_1, u_2, u_3, y) \tag{8}$$

$$kT\chi_s = 4\sum_{r=1}^{\infty} r^2 L_r(u_1, u_2, u_3, y).$$ (9)

The first two Ls can be obtained from the information in figure 4(b) as

$$L_1 = u_1^2 u_2 u_3 \theta_1$$ (10)

$$L_2 = 2u_1^3 u_2^2 u_3^2 + u_1^4 u_2 u_3^2 \theta_2 + u_1^4 u_2^2 u_3 \theta_2 - 2.5 u_1^4 u_2^2 u_3^2 \theta_2 - 2u_1^4 u_2^2 u_3^2$$ (11)

with the notation $\theta_n = (y^n + y^{-n})/2$. Higher order terms are obtained using basically standard methods [20], which involve

(i) computer generation of all bare graphs with r vertices and any number of edges;

(ii) embedding of each graph in the lattice and storage of vertex and edge types in each embedding; and

(iii) accumulation of data for all graphs.

We have obtained the complete L_r multinomials for $r \leqslant 7$. There are a total of 426 bare graphs which contribute to this order. If we wish to group terms by powers of u_1, for example, then some contributions from higher order graphs must also be included. In particular to obtain a series in u_1 through order 8 a partial set of graphs with up to 16 vertices is needed. In the appendix we give the leading parts of the L_r multinomials for $r \leqslant 16$. From these we can then obtain the corresponding series for M_s and χ_s.

3. Analysis and results

The parameters V_i in the lattice-gas Hamiltonian (2) should be regarded as 'effective pair interactions' which can be obtained from a fit to the experimental phase diagram. Hilton *et al* [25] have recently attempted to do this, and the reasonable agreement of their interaction parameters with the first-principles estimates of Sterne and Wille [26] indicates that other interactions not included in the lattice-gas Hamiltonian (2) are of minor importance. In this paper we are not so concerned with modelling the real system, but rather with more general (and more qualitative) aspects and we choose the values (in dimensionless units) $V_1 = 1$, $V_2 = -0.5$, $V_3 = 0.5$. This is the choice made by previous authors [12, 17] and has the virtue that we can directly compare our estimated phase boundary with this previous work. Other choices of the parameters lead to qualitatively similar phase diagrams.

Except for very special choices of the ratios V_2/V_1, V_3/V_1 the expansion variables u_i are not simply related and the series cannot be directly expressed in terms of a single variable. Instead we adopt the following approach: we choose fixed values of u_2, u_3, y and analyse the resulting single variable series in u_1 to find the critical value u_{1c}. By varying the choice of (u_2, u_3) we can find a case where, on the critical line, the desired ratio of Vs holds. In practice we have used the series for the order parameter M_s. In table 1 we give the coefficients of this series for several cases. The series can be analysed by standard Padé approximant methods to yield estimates of u_{1c} and the critical exponent β, which appears to take the universal 2D Ising value $\beta = 1/8$. Assuming this value, more precise estimates of the critical temperature can be obtained from the series for M_s^{-8}. Typical results are shown in table 2.

In this way we have mapped out the phase boundary between the Ortho I and Tetra phases. In figure 5 we show our estimates and, for comparison, the transfer matrix results of Aukrust *et al* [17]. The agreement is excellent.

Table 1. Coefficients of the staggered magnetization series for three choices of parameters, as shown.

$u_2 = 0.3962$	$u_2 = 0.3875$	$u_2 = 0.2435$
$u_3 = 2.5240$	$u_3 = 2.5806$	$u_3 = 4.1068$
$y = 1.0000$	$y = 0.5000$	$y = 0.0250$
1.000 000E0	1.000 000E0	1.000 000E0
0.000 000E0	0.000 000E0	0.000 000E0
−2.000 000E0	−2.500 000E0	−4.002 500E1
−8.000 000E0	−8.000 000E0	−8.000 000E0
−6.683 992E1	−8.274 108E1	−7.263 382E3
−2.403 549E2	−2.924 326E2	−2.850 047E4
−1.392 907E3	−1.732 184E3	1.126 554E5
−6.705 846E3	−9.233 300E3	−9.586 626E6
−3.570 318E4	−4.766 731E4	8.829 626E7

Table 2. Results of Padé approximant analysis of the staggered magnetization series for two cases: (a) uniform chemical potential, $\zeta = 1$; (b) non-uniform chemical potential, $\zeta = 0.95$.

(a)	u_2	u_3	y	u_{1c}	kT/V_1	μ/V_1
	0.3962	2.5240	1.0000	0.1569	0.5400	2.0000
	0.3875	2.5806	0.5000	0.1502	0.5274	1.6344
	0.3718	2.6896	0.3000	0.1382	0.5054	1.3915
	0.3548	2.8185	0.2000	0.1259	0.4825	1.2235
	0.3239	3.0874	0.1080	0.1049	0.4435	1.0129
	0.2784	3.5920	0.0480	0.0775	0.3911	0.8126
	0.2435	4.1068	0.0250	0.0593	0.3540	0.6942
	0.1634	6.1200	0.0060	0.0267	0.2760	0.5878
(b)	u_2	u_3	y	u_{1c}	kT/V_1	μ/V_1
	0.4117	2.4290	1.0000	0.1695	0.5634	2.0000
	0.4023	2.4857	0.5139	0.1618	0.5491	1.6344
	0.3857	2.5927	0.3137	0.1488	0.5249	1.3915
	0.3673	2.7226	0.2110	0.1349	0.4992	1.2234
	0.3351	2.9842	0.1155	0.1123	0.4574	1.0129
	0.2880	3.4722	0.0520	0.0829	0.4017	0.8126
	0.2539	3.9386	0.0279	0.0644	0.3647	0.6942
	0.1700	5.8824	0.0067	0.0289	0.2822	0.5878

4. Uniaxial anisotropy

In our analysis above the sublattices A, B were equivalent. This means that the filled oxygen chains may lie in either of the diagonal directions in figure 1. Experimentally this occurs and leads to twinning. By applying a uniaxial stress during growth, twinning can be avoided or reduced [22–24]. This can be modelled by making the V_2, V_3 interactions anisotropic or, more simply, by choosing a chemical potential which is sublattice-dependent and hence favours one sublattice. We use this latter approach here, and choose $\mu_A = \mu$, $\mu_B = \mu - \delta$, with $\delta > 0$. The atoms will then preferentially occupy sublattice A. In the formulation of our low-temperature expansion this gives $y_A = y$, $y_B = y\zeta^2$, with $\zeta = \exp(-\frac{1}{2}\beta\delta)$. It is straightforward to show that this leads to the substitution in the quantity L_r

$$\theta_n \to \tfrac{1}{2}\zeta^r[(y\zeta)^n + (y\zeta)^{-n}]. \tag{12}$$

Note that this depends on both r and n. Thus, for example

$$L_1 = \tfrac{1}{2}u_1^2 u_2 u_3 (y\zeta^2 + y^{-1})$$
$$L_2 = 2u_1^3 u_2^2 u_3^2 \zeta^2 + \tfrac{1}{2}u_1^4 u_2 u_3^2 (y^2\zeta^4 + y^{-2}) + \cdots.$$

(13)

With this change all of the previous results can be used.

The same method of analysis can be used. In table 2 and figure 5 we present results for the choice $\zeta = 0.95$ which corresponds, roughly, to a 5% decrease in chemical potential on one sublattice. The transition temperature is also found to increase by about 5%. Unfortunately no experimental data seem to be available to check this result.

5. Conclusions

We have developed a low-temperature expansion for the previously studied lattice-gas model of oxygen ordering in $YBa_2Cu_3O_{6+x}$. Because of the rather complex nature of the Hamiltonian this is quite difficult to extend to high order, but we have been able to obtain series for the order parameter and susceptibility in the Ortho I phase, to eighth-order in the 'temperature' variable. Analysis of the resulting series locates the Ortho I–Tetra phase boundary to an accuracy at least equal to that achieved by other methods, and confirms the expected universal Ising nature of the transition [16]. Our results are in excellent agreement with previous studies.

We have also extended our series to the case of a sublattice-dependent chemical potential, to model the case of a uniaxial stress. This leads to an increase in the critical temperature, but a detailed comparison with experiment is not possible at this stage.

Finally we have also attempted to derive a low-temperature expansion in the Ortho II phase but this has been largely unsuccessful, due to the difficulty of finding a suitable expansion variable which does not require contributions from graphs with excessively many overturned spins.

Acknowledgments

Appendix

Leading terms in the quantities $L_r(u_1, u_2, u_3, y)$. For convenience a term of the form $Cu_1^{p_1} u_2^{p_2} u_3^{p_3} \theta_{p_4}$ is represented as $C(p_1, p_2, p_3, p_4)$.

$$L_1 = (2, 1, 1, 1)$$

$$L_2 = 2(3, 2, 2, 0) + (4, 1, 2, 2) + (4, 2, 1, 2) - 2(4, 2, 2, 0) - 2\tfrac{1}{2}(4, 2, 2, 2)$$

$$L_3 = 2(4, 2, 3, 1) + 2(4, 3, 2, 1) + 2(4, 3, 3, 1) + 4(5, 2, 3, 1) + 4(5, 3, 2, 1) - 24(5, 3, 3, 1)$$
$$+ (6, 1, 3, 3) + 4(6, 2, 2, 3) - 6(6, 2, 3, 1) - 8(6, 2, 3, 3) + (6, 3, 1, 3)$$
$$- 6(6, 3, 2, 1) - 8(6, 3, 2, 3) + 22(6, 3, 3, 1) + 10\tfrac{1}{3}(6, 3, 3, 3)$$

$$L_4 = \tfrac{1}{2}(4,2,4,0) + \tfrac{1}{2}(4,4,2,0) + 4(5,3,3,0) + 4(5,3,3,2) + 4(5,3,4,0) + 4(5,4,3,0)$$
$$+ 2(5,4,4,0) + 2(6,2,4,0) + 4(6,2,4,2) + 8(6,3,3,2) - 10(6,3,4,0)$$
$$- 12(6,3,4,2) + 2(6,4,2,0) - 10(6,4,3,0) - 12(6,4,3,2) + 4(6,4,2,2)$$
$$- 45(6,4,4,0) - 16(6,4,4,2) + 2(7,2,4,0) + 4(7,2,4,2) + 4(7,3,3,0)$$
$$+ 20(7,3,3,2) - 32(7,3,4,0) - 72(7,3,4,2) + 2(7,4,2,0) + 4(7,4,2,2)$$
$$- 32(7,4,3,0) - 72(7,4,3,2) + 134(7,4,4,0) + 156(7,4,4,2) + (8,1,4,4)$$
$$+ (8,2,2,4) + 8(8,2,3,4) - 4\tfrac{1}{2}(8,2,4,0) - 8(8,2,4,2) - 16\tfrac{1}{2}(8,2,4,4)$$
$$+ 8(8,3,2,4) - 8(8,3,3,0) - 32(8,3,3,2) - 52(8,3,3,4) + 38(8,3,4,0)$$
$$+ 84(8,3,4,2) + 59(8,3,4,4) + (8,4,1,4) - 4\tfrac{1}{2}(8,4,2,0) - 8(8,4,2,2)$$
$$- 16\tfrac{1}{2}(8,4,2,4) + 38(8,4,3,0) + 84(8,4,3,2) + 59(8,4,3,4) - 91(8,4,4,0)$$
$$- 140(8,4,4,2) - 52\tfrac{1}{4}(8,4,4,4)$$

$$L_5 = 4(5,3,4,1) + 4(5,4,3,1) + 2(6,2,5,1) + (6,3,3,3) + 6(6,3,4,1) - 6(6,3,5,1)$$
$$+ 6(6,4,3,1) + 24(6,4,4,1) + 6(6,4,5,1) + 2(6,5,2,1) - 6(6,5,3,1)$$
$$+ 6(6,5,4,1) + 2(6,5,5,1) + 12(7,3,4,1) + 12(7,3,4,3) + 24(7,3,5,1)$$
$$+ 12(7,4,3,1) + 12(7,4,3,3) - 72(7,4,4,1) - 40(7,4,4,3) - 136(7,4,5,1)$$
$$+ 24(7,5,3,1) - 136(7,5,4,1) - 112(7,5,5,1) + 6(8,2,5,1) + 6(8,2,5,3)$$
$$+ 4(8,3,3,3) + 8(8,3,4,1) + 24(8,3,4,3) - 84(8,3,5,1) - 60(8,3,5,3)$$
$$+ 8(8,4,3,1) + 24(8,4,3,3) - 64(8,4,4,1) - 104(8,4,4,3) - 24(8,4,5,1)$$
$$+ 50(8,4,5,3) + 6(8,5,2,1) + 6(8,5,2,3) - 84(8,5,3,1) - 60(8,5,3,3)$$
$$- 24(8,5,4,1) + 50(8,5,4,3) + 1118(8,5,5,1) + 120(8,5,5,3) + \cdots$$

$$L_6 = 2(5,4,4,0) + 2(6,3,4,2) + 4(6,3,5,0) + 12(6,4,4,0) + 8(6,4,4,2) + 2(6,4,3,2)$$
$$+ 4(6,4,5,0) + 4(6,5,3,0) + 4(6,5,4,0) + 4(7,3,5,0) + 12(7,3,5,2)$$
$$+ 4(7,3,6,0) + 12(7,4,4,0) + 20(7,4,4,2) - 16(7,4,5,0) - 24(7,4,5,2)$$
$$- 14(7,4,6,0) + 4(7,5,3,0) - 16(7,5,4,0) - 24(7,5,4,2) + 12(7,5,3,2)$$
$$+ 36(7,5,5,0) + 12(7,5,5,2) + 8(7,5,6,0) + 4(7,6,3,0) - 14(7,6,4,0)$$
$$+ 8(7,6,5,0) + 2(7,6,6,0) + 2(8,2,6,0) + 3(8,2,6,2) + 4(8,3,4,4)$$
$$+ 8(8,3,5,0) + 20(8,3,5,2) - 12(8,3,6,0) - 24(8,3,6,2) + 4(8,4,3,4)$$
$$+ 8(8,4,4,0) + 25(8,4,4,2) - 12(8,4,4,4) - 12(8,4,5,0) + 8(8,4,5,2)$$
$$+ 42(8,4,6,0) + 36(8,4,6,2) + 8(8,5,3,0) + 20(8,5,3,2) - 12(8,5,4,0)$$
$$+ 8(8,5,4,2) - 432(8,5,5,0) - 448(8,5,5,2) - 276(8,5,6,0)$$
$$- 106(8,5,6,2) + 2(8,6,2,0) + 3(8,6,2,2) - 12(8,6,3,0) - 24(8,6,3,2)$$
$$+ 36(8,6,4,2) + 42(8,6,4,0) - 276(8,6,5,0) - 106(8,6,5,2)$$
$$- 132(8,6,6,0) - 46(8,6,6,2) + \cdots$$

$$L_7 = (6,3,5,1) + 4(6,4,4,1) + 8(6,4,5,1) + (6,5,3,1) + 8(6,5,4,1) + 8(7,4,4,1)$$
$$+ 8(7,4,4,3) + 44(7,4,5,1) + 8(7,4,6,1) + 44(7,5,4,1) + 8(7,5,5,1)$$
$$+ 4(7,5,6,1) + 8(7,6,4,1) + 4(7,6,5,1) + 2(8,3,5,1) + 8(8,3,5,3)$$
$$+ 20(8,3,6,1) + 6(8,3,7,1) + 8(8,4,4,3) + 34(8,4,5,1) + 6(8,4,5,3)$$
$$- 20(8,4,6,1) - 18(8,4,7,1) + 2(8,5,3,1) + 8(8,5,3,3) + 34(8,5,4,1)$$
$$+ 6(8,5,4,3) - 186(8,5,5,1) - 74(8,5,5,3) - 194(8,5,6,1) - 12(8,5,7,1)$$
$$+ 20(8,6,3,1) - 20(8,6,4,1) - 194(8,6,5,1) + 80(8,6,6,1) + 10(8,6,7,1)$$
$$+ 6(8,7,3,1) - 18(8,7,4,1) - 12(8,7,5,1) + 10(8,7,6,1) + 2(8,7,7,1) + \cdots$$

$$L_8 = 2(6,4,5,0) + (6,4,6,0) + 2(6,5,4,0) + (6,6,4,0) + 2(7,4,4,0) + 8(7,4,5,0)$$
$$+ 16(7,4,5,2) + 6(7,4,6,0) + 8(7,5,4,0) + 16(7,5,4,2) + 40(7,5,5,0)$$
$$+ 16(7,5,5,2) + 8(7,5,6,0) + 6(7,6,4,0) + 8(7,6,5,0) + 2(8,3,6,0)$$
$$+ 4(8,3,6,2) + (8,3,8,0) + 2(8,4,4,4) + 6(8,4,5,0) + 20(8,4,5,2)$$
$$+ 16(8,4,6,0) + 12(8,4,6,2) + 4(8,4,7,0) - 3\tfrac{1}{4}(8,4,8,0) + 6(8,5,4,0)$$
$$+ 20(8,5,4,2) + 44(8,5,5,0) + 80(8,5,5,2) + 18(8,5,6,0) - 48(8,5,6,2)$$
$$+ 12(8,5,7,0) + 2(8,6,3,0) + 4(8,6,3,2) + 16(8,6,4,0) + 12(8,6,4,2)$$
$$+ 18(8,6,5,0) - 48(8,6,5,2) - 43(8,6,6,0) + 16(8,6,6,2) + 4(8,6,7,0)$$
$$+ 4(8,7,4,0) + 12(8,7,5,0) + 4(8,7,6,0) - 3\tfrac{1}{4}(8,8,4,0) + 8(8,8,3,0) + \cdots$$

$$L_9 = (6,5,5,1) + 4(7,4,5,1) + 8(7,4,6,1) + 4(7,5,4,1) + 32(7,5,5,1) + 8(7,5,6,1)$$
$$+ 8(7,6,4,1) + 8(7,6,5,1) + 4(8,4,5,1) + 6(8,4,5,3) + 24(8,4,6,1)$$
$$+ 6(8,4,7,1) + 4(8,5,4,1) + 6(8,5,4,3) + 104(8,5,5,1) + 40(8,5,5,3)$$
$$+ 100(8,5,6,1) - 2(8,5,7,1) + 24(8,6,4,1) + 100(8,6,5,1) + 104(8,6,6,1)$$
$$+ 8(8,6,7,1) + 6(8,7,4,1) - 2(8,7,5,1) + 8(8,7,6,1) + \cdots$$

$$L_{10} = 2(7,4,6,0) + 4(7,5,5,0) + 4(7,5,5,2) + 8(7,5,6,0) + 2(7,6,4,0) + 8(7,6,5,0)$$
$$+ 2(7,6,6,0) + 2(8,4,5,2) + 6(8,4,6,0) + 5(8,4,6,2) + 2(8,5,4,2)$$
$$+ 24(8,5,5,0) + 32(8,5,5,2) + 72(8,5,6,0) + 64(8,5,6,2) + 24(8,5,7,0)$$
$$+ 6(8,6,4,0) + 5(8,6,4,2) + 72(8,6,5,0) + 64(8,6,5,2) + 40(8,6,6,0)$$
$$+ 3(8,6,6,2) + 8(8,6,7,0) + 24(8,7,5,0) + 8(8,7,6,0) + \cdots$$

$$L_{11} = 4(7,5,6,1) + 4(7,6,5,1) + 4(8,4,6,1) + 8(8,5,5,1) + 64(8,5,6,1) + 24(8,5,7,1)$$
$$+ 6(8,5,5,3) + 4(8,6,4,1) + 64(8,6,5,1) + 88(8,6,6,1) + 12(8,6,7,1)$$
$$+ 24(8,7,5,1) + 12(8,7,6,1) + \cdots$$

$$L_{12} = 2(7,6,6,0) + \tfrac{1}{2}(8,4,6,0) + 10(8,5,6,0) + 12(8,5,6,2) + 12(8,5,7,0) + 2(8,5,8,0)$$
$$+ 10(8,6,5,0) + \tfrac{1}{2}(8,6,4,0) + 12(8,6,5,2) + 52(8,6,6,0) + 16(8,6,6,2)$$

$$+ 4(8,6,7,0) + (8,6,8,0) + 12(8,7,5,0) + 4(8,7,6,0) + 2(8,8,5,0)$$
$$+ (8,8,6,0) + \cdots$$

$$L_{13} = 2(8,5,6,1) + 4(8,5,7,1) + 2(8,6,5,1) + 32(8,6,6,1) + 12(8,6,7,1) + 12(8,7,6,1)$$
$$+ 4(8,7,5,1) + \cdots$$

$$L_{14} = 4(8,6,6,0) + 2(8,6,6,2) + 8(8,6,7,0) + 8(8,7,6,0) + \cdots$$

$$L_{15} = 2(8,6,7,1) + 2(8,7,6,1) + 2(8,7,7,1) + \cdots$$

$$L_{16} = \tfrac{1}{2}(8,6,8,0) + \tfrac{1}{2}(8,8,6,0) + \cdots.$$

References

[1]   Jorgenen J D, Beno M A, Hinks D G, Soderholm L, Volin K J, Hitterman R L, Grace J D, Schuller I K, Segre C U, Zhang K and Kleefisch M Sl 1987 *Phys. Rev.* B **36** 3608
[2]   Cava R J, Batlogg B, Chen C H, Rietman E A, Zahurak S M and Werder D 1987 *Phys. Rev.* B **36** 5719
[3]   Poulsen H F, Andersen N H, Andersen J V, Bohr H and Mouritsen O G 1991 *Nature* **349** 594
[4]   de Fontaine D, Wille L T and Moss S C 1987 *Phys. Rev.* B **36** 5709
[5]   Wille L T and de Fontaine D 1988 *Phys. Rev.* B **37** 2227
[6]   Khachaturyan A G and Morris J W Jr 1987 *Phys. Rev. Lett.* **59** 2776; 1988 *Phys. Rev. Lett.* **61** 215
[7]   Aligia A A, Bonadeo H and Garces J 1991 *Phys. Rev.* B **43** 542
[8]   Zubkus V E, Tornau E E, Lapinskas S and Kundrotas P J 1991 *Phys. Rev.* B **43** 13 112
[9]   Wille L J, Berera A and de Fontaine D 1988 *Phys. Rev. Lett.* **11** 1065
[10] Cai Z X and Mahanti S D 1988 *Solid State Commun.* **67** 287
[11] de Fontaine D, Mann M E and Ceder G 1989 *Phys. Rev. Lett.* **63** 1300
[12] Burmester C P and Wille L 1989 *Phys. Rev.* B **40** 8795
[13] Wille L T 1989 *Phys. Rev.* B **40** 6931
[14] Berera A and de Fontaine D 1989 *Phys. Rev.* B **39** 6727
[15] Kikuchi R and Choi J S 1989 *Physica* C **160** 347
[16] Bartelt N C, Einstein T L and Wille L T 1989 *Phys. Rev.* B **40** 10 759
[17] Aukrust T, Novotny M A, Rikvold P A and Landau D P 1990 *Phys. Rev.* B **41** 8772
[18] de Fontaine D, Ceder G and Asta M 1990 *Nature* **343** 544
[19] Adelman D, Burmester C P, Wille L T, Sterne P A and Gronsky R 1992 *J. Phys. C: Solid State Phys.* 4 L585
[20] Domb C 1974 *Phase Transitions and Critical Phenomena* vol 3, ed C Domb and M S Green (New York: Academic)
[21] Slawny J 1979 *J. Stat. Phys.* **20** 711
[22] Schmid H, Burkhardt E, Sun B N and Rivera J P 1989 *Physica* C **157** 555
[23] Kaiser D L, Gayle F W, Roth R S and Swartzendruber L J 1989 *J. Mater. Res.* 4 745
[24] Liu J Z, Lau M D, Klavins P and Shelton R N 1990 *Phys. Lett.* **144A** 265
[25] Hilton D K, Gorman B M, Rikvold P A and Novotny M A 1992 *Phys. Rev.* B **46** 381
[26] Sterne P A and Wille L T 1989 *Physica* C **162** 223